OXFORD

Cerebral Cortex, 2023, **33**, 9566–9582
https://doi.org/10.1093/cercor/bhad227
Advance access publication date 29 June 2023
Original Article

Highly branched and complementary distributions of layer 5 and layer 6 auditory corticofugal axons in mouse

Lina K. Issa[1,2,†], Nathiya V.C. Sekaran[1,2,†], Daniel A. Llano[1,2,3,4,*]

[1]Department of Molecular and Integrative Physiology, University of Illinois at Urbana—Champaign, Champaign, IL, United States,
[2]Beckman Institute for Advanced Science and Technology, Urbana, IL, United States,
[3]Department of Biomedical and Translational Sciences, Carle Illinois College of Medicine, Urbana, IL, United States,
[4]Department of Speech and Hearing Science, University of Illinois at Urbana-Champaign, Champaign, IL, United States

*Corresponding author: Email: d-llano@illinois.edu
[†]Lina K. Issa and Nathiya V.C. Sekaran contributed equally.

The auditory cortex exerts a powerful, yet heterogeneous, effect on subcortical targets. Auditory corticofugal projections emanate from layers 5 and 6 and have complementary physiological properties. While several studies suggested that layer 5 corticofugal projections branch widely, others suggested that multiple independent projections exist. Less is known about layer 6; no studies have examined whether the various layer 6 corticofugal projections are independent. Therefore, we examined branching patterns of layers 5 and 6 auditory corticofugal neurons, using the corticocollicular system as an index, using traditional and novel approaches. We confirmed that dual retrograde injections into the mouse inferior colliculus and auditory thalamus co-labeled subpopulations of layers 5 and 6 auditory cortex neurons. We then used an intersectional approach to relabel layer 5 or 6 corticocollicular somata and found that both layers sent extensive branches to multiple subcortical structures. Using a novel approach to separately label layers 5 and 6 axons in individual mice, we found that layers 5 and 6 terminal distributions partially spatially overlapped and that giant terminals were only found in layer 5-derived axons. Overall, the high degree of branching and complementarity in layers 5 and 6 axonal distributions suggest that corticofugal projections should be considered as 2 widespread systems, rather than collections of individual projections.

Key words: thalamus; inferior colliculus; midbrain; FOXP2; RBP4.

Introduction

The sensory regions of the cerebral cortex send dense and extensive projections to subcortical structures. These descending projections emanate from layers 5 (L5) and 6 (L6) of the cerebral cortex and play a number of important roles, such as facilitating predictive coding, mediating synaptic plasticity at subcortical targets, and permitting escape responses (for review see Asilador and Llano 2021). Classically, L5 sends sparse, but large, terminals to the thalamus and has more extensive projections to the midbrain, with less well-characterized projections to other structures such as to the corpus striatum, amygdala, or hindbrain regions. L6 has well-established extensive projections to thalamus, consisting of small terminals on distal dendrites, and has been referred to as having a role to modulate the activity, rather than driving spiking activity on its own, in thalamic targets (reviewed in Sherman 2011). Recent work has expanded the range of targets of L6 corticofugal targets, particularly in the auditory system, such that L6 of the auditory cortex (AC) has been shown to project to striatum, inferior colliculus (IC), and superior colliculus (SC; Schofield 2009; Slater et al. 2013, 2019; Rock et al. 2016; Zurita et al. 2018; Ponvert and Jaramillo 2019).

The question of whether the extensive descending projections from L5 or L6 are branched to innervate multiple targets is an important and unanswered one. Branching allows a single message to be broadcast to multiple brain regions, which is an effective means of synchronizing activity across multiple levels of nervous system, modulating activity globally (e.g., analogous to monoaminergic ascending branching systems) or sending a copy of a signal from one brain region to another. Previous authors have speculated that L5 sensory corticothalamic axons are branches from longer projections that mediate motor outflow (Sherman and Usrey 2021). As a consequence, L5 projections to thalamus have been speculated to be involved in an efferent copy system, allowing motor commands to modify sensory processing. This supposition is supported by studies showing that L5 corticothalamic projections branch to midbrain or brainstem targets in the visual and somatosensory systems (Deschênes et al. 1994; Bourassa et al. 1995; Bourassa and Deschênes 1995) and that sensory L5 neurons branch to striatum and/or amygdala (Donoghue and Kitai 1981; Moriizumi and Hattori 1991; Asokan et al. 2018). In addition, L5 axons appear particularly well suited to send synchronized messages to multiple brain regions given their thick axons and tendency to send information in "packets" of bursts of spikes (Wang and McCormick 1993; Kasper et al. 1994; Rumberger et al. 1998; Christophe et al. 2005; Slater et al. 2013, 2019). However, other work has suggested that the sensory L5 system comprises multiple subsystems and that each L5 subcortical target is at least partially derived from a separate group of L5 neurons (Doucet et al. 2002, 2003; Hattox and Nelson 2007). The scenario in L6 is less well understood. Sensory L6 neurons densely innervate the thalamus and thalamic reticular nucleus (TRN) and these projections emanate from all depths of L6 (Kim et al. 2014; Hoerder-Suabedissen et al. 2018). L6 corticothalamic neurons are thought to play an important role in adjusting tuning of sensory thalamic neurons (reviewed in Antunes and Malmierca 2021).

Received: January 16, 2023. **Revised:** June 5, 2023. **Accepted:** June 6, 2023

As outlined above, auditory L6 descending projections to non-thalamic targets were only recently revealed, and they generally appeared to emanate very deeply in L6 and are either non-pyramidal or are pyramidal with a flattened orientation (Schofield 2009; Slater et al. 2013; Zurita et al. 2018), prompting speculation that they comprise a population of neurons independent from L6 corticothalamic neurons (Asilador and Llano 2021).

Part of the challenge in interpreting branching studies is that the most common approach to test for branching axons is to inject two retrograde tracers into the two putative targets of a particular pathway and to measure the proportion of double retrogradely labeled cells. Although the presence of double-labeled cells with this approach is highly suggestive of branching, there are several problems with this method. First, if an axon branches to innervate multiple targets, each branch likely innervates only a portion of the target structure, such that if the two injections miss the "matched" regions of the two putative targets, only one label will be taken up by the branched axon. Second, it is possible that the presence of one tracer may impact the ability of the other tracer to travel. Indeed, previous work done injecting two retrograde tracers into identical sites into a target structure has revealed a sensitivity of 4–70% of identifying double-labeled cells (Schofield et al. 2007). This percentage would presumably decrease when injecting into two structures with topographically mismatched injections. A gold standard approach to examine for branching would be to label a very small number of neurons via intra- or juxtacellular injections and reconstruct the axonal pathway (Deschênes et al. 1994; Bourassa et al. 1995; Bourassa and Deschênes 1995), but this is highly labor-intensive and produces a small yield of labeled neurons.

Therefore, in the current study, we used an intersectional approach to study branching in both L5 and L6 descending projections emanating from one of the largest and most diverse auditory corticofugal projections—the corticocollicular projection. We first used traditional dual retrograde approaches to confirm that a small percentage of AC L5 and L6 neurons branch to the medial geniculate body (MGB) and IC. We then used a Cre-specific retrograde flippase-inducing canine-adenovirus to induce flippase in RBP4-expressing AC neurons to label L5 (Kozorovitskiy et al. 2012; Glickfeld et al. 2013) or FOXP2-expressing AC neurons to label L6 (Ferland et al. 2003) corticocollicular neurons. We then refilled flippase-expressing neurons with a flippase-dependent fluorophore and observed widespread branching to subcortical structures from the two layers. Finally, we developed a novel intersectional approach to label L5 and L6 with different fluorophores in the same mouse using a single AC injection site to directly compare L5 and L6 innervation patterns in their various target structures. We observed that in brain regions with both L5 and L6 innervation, the two show complementary and partially overlapping patterns in terms of geographic distribution of terminals and terminal size. This work suggests that the L5 and L6 systems show a much greater degree of branching than previously suggested and that terminals from these two layers retain distinct profiles in their subcortical targets.

Materials and methods

Mice

For dual retrograde injection experiments, male and female 3–6-month-old CBA/CaJ mice were used. For all other experiments, either FOXP2-Cre (B6.Cg-Foxp2tm1.1(cre)Rpa/J, from The Jackson Laboratory, stock #030541), RBP4-Cre (Tg(Rbp4-cre)KL100Gsat/Mmucd from the Mutant Mouse Resource and Research Center, stock #031125-UCD), or neurotensin receptor 1 (NTSR1)-Cre (MMRRC, 017266-UCD) mice were used. These mice are on a C57 background, were 2–3 months old at injection, were bred in-house, and both male and female mice were used. Before the experiments, mice were genotyped using Transnetyx (transnetyx.com), using the following sequences. For FOXP2, 13007 Mutant Reverse A IRES, ACACCGGCCTTATTCCAAG, and 36567 Common, TCCGGAGTTAGAAGATGACAGA were used. For RBP4, forward GGGCGGCCTCGGTCCTC and reverse CGGCAAACGGACAGAAGCATT were used. For NTSR1, forward TTAATCCATATTGGCAGAACGAAAACG and reverse CAGGC-TAAGTGCCTTCTCTACA were used. All animal procedures were approved by the Institutional Animal Care and Use Committee at the University of Illinois at Urbana—Champaign. Mice were housed in animal care facilities approved by the Association for Assessment and Accreditation of Laboratory Animal Care International. Every attempt was made to minimize the number of animals used and to reduce suffering at all stages of the experiments.

Surgeries

For dual retrograde tracer experiments, mice were anesthetized with isoflurane (4% induction, 1–2% maintenance) and placed into a stereotaxic frame (Kopf Model 940). Pressure injections of 1% fluorogold (FG, Fluorochrome) in phosphate-buffered saline (PBS) were made into the IC and 1% cholera toxin B (CTB) dissolved in PBS (List chemicals, #104) injected into the MGB. Injection volumes ranged from 50 to 100 nL and were performed using glass pipettes 10–20 μm in diameter backfilled with mineral oil and injected using a Nanoject III device at a rate of 30 nL/min. IC injection coordinates were 1.2 mm posterior to lambda, 1.2 mm lateral to midline, and injections were made from 500 to 1,500 μm deep. MGB injection coordinates were 3.0 mm posterior to bregma, 2.0 mm lateral to midline, and 2,500–2,800 μm deep. After 7 days, mice were transcardially perfused for histological processing.

For intersectional labeling of FOXP2+ or RBP4+ neurons, mice were prepared as above. In a single surgical session, mice were injected in the IC with 100–200 nL of Cav-FlxFlp (6.3E12 GC/mL, https://plateau-igmm.pvm.cnrs.fr/) at a rate of 30 nL/min, which travels in a retrograde Cre-dependent manner to induce flippase production in Cre-expressing neurons. Two IC injections were made: both at 1.2 mm posterior to bregma, with one injection 0.8 mm lateral and another 1.4 mm lateral to midline, at depths of 500–1,500 μm. During the same surgery, flp-dependent mCherry (2E13 GC/mL, AAV9-Ef1a-fDIO-mCherry, Addgene 114471) was injected at 2 sites in the AC (1.3 and 1.7 mm anterior to lambdoid suture at the temporal ridge) at depths of 500–1,000 μm and an angle of 40 degrees from the sagittal plane. Mice were euthanized at 8–10 weeks for histological processing.

To confirm that mCherry-filled cells in the AC were indeed corticofugal neurons (and not trans-synaptically labeled cortical cells), FG (1% in PBS) was injected into the IC in a subset of animals already injected with Cav-FlxFlp and AAV9-Ef1a-fDIO-mCherry. This approach permits a direct comparison of cells retrogradely labeled using the two different approaches. For these injections, FG was injected into the IC at a total volume of 100 nL at a rate of 30 nL/min at the same sites targeted with Cav-FlxFlp. FG was injected one week prior to the animal being euthanized.

For dual labeling of L5 and L6 neurons, FOXP2+ mice were prepared for surgery as described above. pAAV-EF1a-Flpo, retrograde (1E12 GC/mL, Addgene 55637, referred to here as AAVrg, also known as rAAV2-retro), previously established to travel retrogradely and to avoid L6 (Tervo et al. 2016;

Kirchgessner et al. 2021), was injected into the IC. Two IC injections were made: both at 1.2 mm posterior to bregma, with one injection 0.8 mm lateral and another 1.4 mm lateral to midline, at depths of 500–1,500 μm for a total injectate of 200 nL at a rate of 30 nL/min. During the same surgery, in the same pipette a combination of AAV2-pCAG-FLEX-eGFP-WPRE (2.5E12 GC/mL, Addgene 51502) and flp-dependent mCherry (2E13 GC/mL, AAV9-Ef1a-fDIO-mCherry, Addgene 114471) was injected at 2 sites in the AC (1.3 and 1.7 mm anterior to lambdoid suture at the temporal ridge) at depths of 500–1,000 μm and an angle of 40 degrees from the sagittal plane. Mice were euthanized at 8–10 weeks for histological processing.

To determine if L6 neurons also expressed NTSR1, which is expressed in L6 auditory corticothalamic neurons (Guo et al. 2017; Clayton et al. 2021; Ibrahim et al. 2021), 3-month-old male NTSR1-Cre mice were injected with FG in the IC in an identical manner as above. During the same surgery, 100 nL AAV9-FLEX-tdTomato (1.9E13 GC/mL, Addgene 28306) was injected into the AC at the same locations as described above. Mice were euthanized at 12 days for histological processing.

Histological processing, imaging, and processing

Under ketamine (100 mg/kg) and xylazine (3 mg/kg) anesthesia, mice were transcardially perfused with PBS followed by 4% paraformaldehyde in PBS. Brains were extracted, cryoprotected with ascending sucrose gradient up to 30% in PBS (w/v), and frozen-sectioned at 50 μm. Selected sections were immunostained for glutamic acid decarboxylase-67 (GAD-67, 1:1000 Millipore-Sigma MAB5406) to delineate GABAergic modules or the TRN, calretinin (CR, 1:500 Swant, #7697) to delineate MGB subdivisions, CTB (1:500 List labs #703) to visualize CTB-labeled retrogradely filled neurons, complexin-3 to label subplate neurons (1:500, Synaptic systems #122302), or COUP-TF interacting protein 2 (Ctip2) to label infragranular neurons (1:500, Abcam #18465). For immunostaining, floating sections were microwaved at full power for 10–15 s for antigen retrieval, incubated in 0.3% Triton-X in PBS (PBT) followed by 3% normal serum in PBT, then incubated overnight at 4°C in primary antibody. 48-hour incubation was used for CTB primary antibody. After washing in PBT, sections were incubated in secondary antibody (1:500 goat anti-rabbit IgG conjugated to Alexa 405 or 488, for CR, 1:500 goat anti-mouse IgG conjugated to Alexa 405 or 488, for GAD-67, 1:200 for donkey anti-goat Alexa Fluor 555 for CTB, Alexa Fluor 568-conjugated goat anti-rabbit IgG for complexin-3, Alexa Fluor 568-conjugated goat anti-rat IgG for Ctip2, all from ThermoFisher). Sections were coverslipped with Vectashield mounting medium using DAPI except in instances where immunostaining for CR or GAD-67 was done using Alexa 405 or in experiments involving FG injection.

Confocal images were obtained using a Confocal Zeiss LSM 710 Microscope using a 40X objective and tile scan function, with the exception of terminal measurements, which were made using a 63X objective on a Leica-SP8 confocal microscope. Blue-colored images were obtained with 405 nm laser and emission at 415–492 nm. Green-colored images were obtained with 488 nm laser and emission at 491–561 nm. Red-colored images were obtained with 561 nm laser with emission 565–735 nm. For terminal size analysis, maximal-intensity images were obtained at 63X and imported into ImageJ. As we have done previously (Llano and Sherman 2008; Yudintsev et al. 2021), three square regions of area 2,500 μm^2 were placed over each analyzed brain region in the regions of highest joint labeling for sampling. Terminals were traced with the ellipse function in ImageJ (imagej.nih.gov), which automatically calculated terminal area.

To quantify the density of axonal labeling in structures targeted by the L5 and L6 corticofugal systems, images were taken at 10X were taken through all ipsilateral coronal sections that contained any terminal labeling. Regions of interest based on the Allen Brain Institute coronal mouse brain atlas (https://mouse.brain-map.org) were defined. Each region of interest that contained axonal label was thresholded using an adaptive local threshold algorithm in Fiji (https://fiji.sc/), and the number of labeled pixels was counted. For each brain region in each animal, the percentage of total labeled terminals in any given brain region was then calculated.

In cases where debris or embedding medium are present adjacent to tissue sections, a black mask was placed over the debris or embedding medium. In mCherry-labeled sections, either DAPI counterstain or immunostain for GAD or CR is used to outline anatomical borders. In images of control sections where no mCherry terminals were found, DAPI overlays are not shown so that the images can be more easily inspected for lack of mCherry label.

Statistical analysis

Pairwise differences were analyzed using nonparametric statistical tests. Mann–Whitney testing was used to compare the terminal sizes from L5 vs. L6 projections. Two-way ANOVA to examine target region by layer of origin interactions used target region and layer of origin as fixed factors and was run in SPSS. *P*-values of <0.05 were taken as statistically significant.

Results

Both L5 and L6 neurons branch to MGB and IC

Four adult CBA/CaJ mice (age range 3–6 months, 2 males) received injections of FG to the IC and CTB to the MGB (Fig. 1A). No attempt was made to isolate injections to particular subregions of each nucleus. See Fig. 1B and C for representative injection sites. As we and others have shown (Schofield 2009; Slater et al. 2013, 2019; Yudintsev et al. 2021), FG injections to the IC retrogradely label primarily L5 neurons in the AC, whereas a minority (~20–25%) of labeled neurons are in lower L6 (Fig. 1D). Conversely, as has also been previously shown (Ojima 1994; Llano and Sherman 2008), injection of a retrograde tracer into MGB retrogradely labels neurons primarily in L6 of the AC, and a minority of labeled cells are in L5 (Fig. 1E). Overlay of these two images indicates that a small number of cells in each layer were double-labeled with both CTB and FG (Fig. 1F). Quantification of the proportion of double-labeled cells revealed that a minority of neurons were double-labeled. In each case, the layer that had a smaller number of retrogradely labeled neurons at baseline (L5 corticothalamic and L6 corticocollicular) had larger proportions of double-labeled cells, but did not differ from each other (L5 corticothalamic = 25.5% (SD 6.9%, total cells = 1,706, double-labeled cells = 488), L6 corticocollicular 27.6% (SD 7.7%, total cells = 2,948, double-labeled cells = 842), $n = 4$, $p = 0.772$). Layers that had the dominant numbers of retrogradely labeled neurons at baseline (L5 corticocollicular and L6 corticothalamic) had small numbers of double-labeled cells that also did not differ from each other (L5 corticocollicular = 6.7% (SD 8.1%, total cells = 5,617, double-labeled cells = 488), L6 corticothalamic 6.0% (SD 3.2%, total cells = 12,451, double-labeled cells = 842), $n = 4$, $p = 0.486$). Although these data suggest that a minority of neurons were double-labeled, previous work

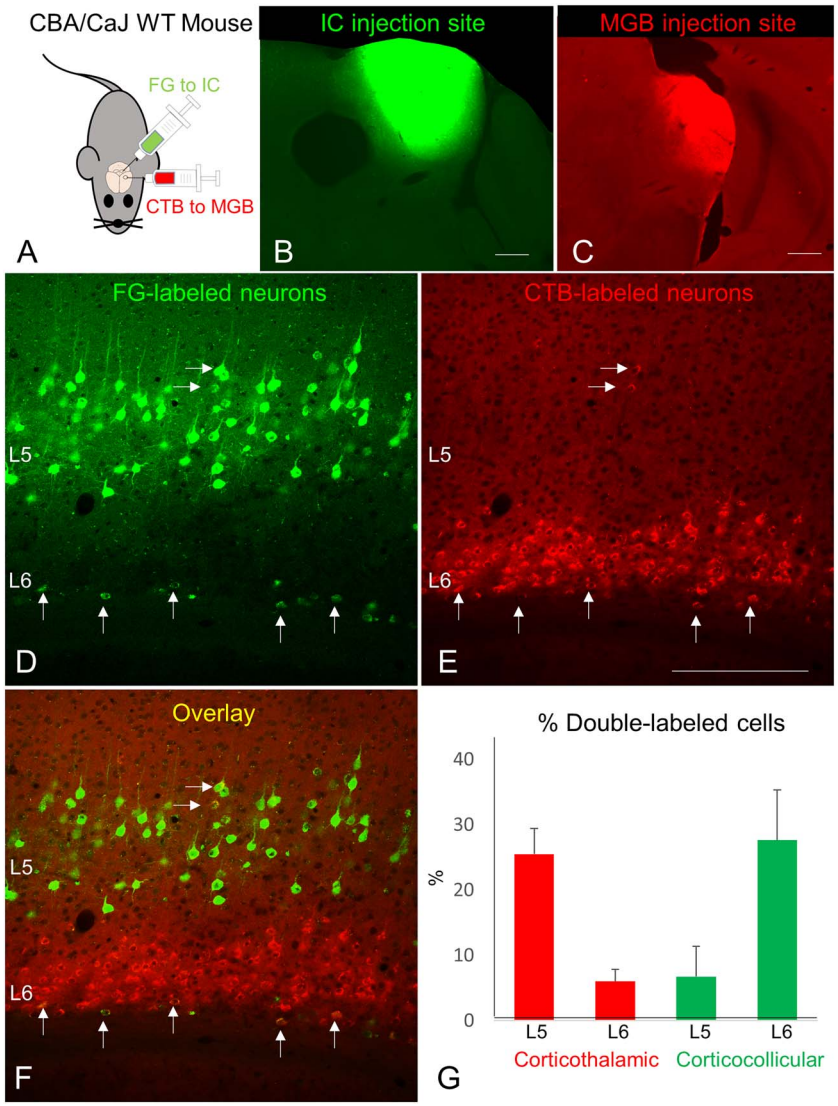

Fig. 1. Demonstration of double-labeled corticothalamic and corticocollicular neurons in both L5 and L6 of AC. A) Diagram of experimental setup. CBA/CaJ mice received injections of FG to the IC and CTB to the MGB. B, C) Representative examples of injection sites into the IC and MGB, respectively. D, E) Representative section through the AC showing retrogradely filled corticocollicular cells and corticothalamic cells in L5 and L6. F) Overlay of D and E showing double-labeled cells in L5 (horizontal arrows) and L6 (vertical arrows). G) Percentage of double-labeled cells seen in each layer and each cell type in $n = 4$ mice. Note that the maximum expected possible % of double-labeled cells was empirically determined in this study to be 55.3%. Scale bar = 250 μm.

has shown that the approach of dual retrograde labeling double-labels only a small proportion of neurons, even when tracers are injected into the same location, depending on the tracers used (Schofield et al. 2007). We have repeated this control with FG and CTB both injected into identical sites in the IC and found that 55.3% (445/804) of neurons were double-labeled. Therefore, the numbers of double-labeled neurons should be taken as underestimate of branching, and only indicate that branching exists.

L5 corticocollicular neurons branch extensively to subcortical sites

To determine which other brain regions receive branching terminals from L5 corticocollicular axons, injections of a Cre-dependent retrograde tracer that induces flippase expression (Cav-FlxFlp) were made into the IC of 8 mice (5 female) that expressed Cre-recombinase in RBP4+ neurons, which are found in L5 (Fig. 2A, $n = 4$). Terminals of the labeled projections were found in the IC as expected, as this was the initial source of retrograde virus injection (Fig. 2B), and most terminals were in the nonlemniscal portions of the IC (dorsal cortex (DC) and lateral cortex (LC)). To identify GABAergic modules in the lateral cortex, sections were immunolabeled for GAD-67. As previously shown (Lesicko et al. 2016), terminals were found primarily outside of the GABAergic modules in the matrix of the LC (Fig. 2B). mCherry-filled neurons in the AC were large pyramidal cells in L5 with long apical dendrites (Fig. 2C). Quantification of the degree of specificity of the label to L5 revealed that this approach labels nearly exclusively L5 neurons in the AC (97.6% labeled neurons in L5, Fig. 2D). In mice that also had FG injected into the IC, mCherry-filled L5 neurons were found to be a subset of FG-labeled neurons in L5, but not L6 (Fig. 2E). In RBP4-Cre animals without Cav-FlxFlp injected into the IC but with AAV9-Ef1a-fDIO-mCherry into the AC, no AC label was seen (Fig. 2F). No label was also seen in wild-type mice injected with both Cav-FlxFlp to IC and AAV9-Ef1a-fDIO-mCherry to AC (data not shown).

A survey of other brain regions revealed mCherry+ terminals in the MGB, primarily in the dorsal (MGd) and medial (MGm) subdivisions (delineated from ventral division, MGv, by CR

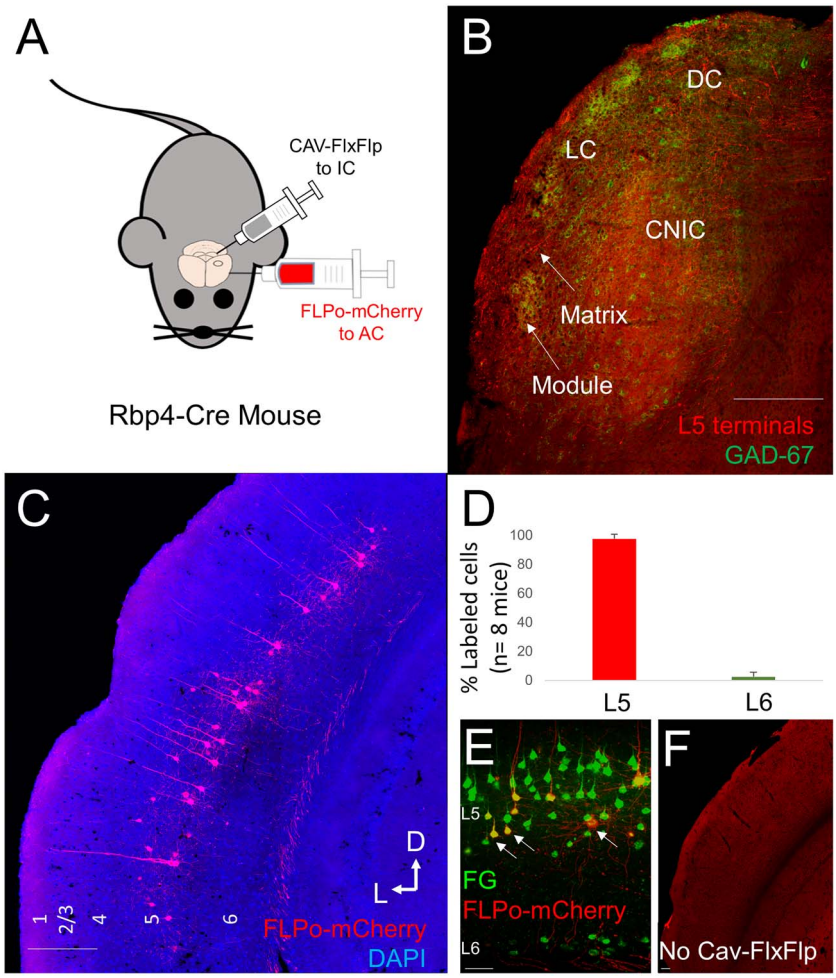

Fig. 2. Experimental setup for examination of L5 corticocollicular branches. A) RBP4-Cre mice were injected with a combination of Cav-FlxFlp in the IC to induce flippase expression in RBP4+ corticocollicular neurons. The mice were also injected with Flpo-mCherry to induce mCherry expression in the flippase-labeled cells. B) Micrograph of the resulting labeling in the IC showing mCherry terminals in the expected regions, primarily LC and DC, and primarily in the GAD-67 poor matrix of the LC. Scale bar = 250 μm. C) Retrogradely labeled neurons in L5 of the AC. Scale bar = 300 μm. D) Proportion of L5-labeled vs. L6-labeled cells in the AC across $n = 8$ animals. E) FG-retrogradely labeled cells after IC injection double-labeled with mCherry only in L5 of RBP4-Cre animals. Double-labeled cells are denoted with white arrows. F) AC of RBP4-Cre animal injected with Flpo-mCherry but not Cav-FlxFlp showing no signal. Scale bar for e and f = 100 μm. CNIC, central nucleus of the inferior colliculus.

immunostaining) as well as adjacent areas corresponding to the reported locations of the suprageniculate nucleus (SG), paralaminar nuclei, and peripeduncular nucleus (PP; Fig. 3A). mCherry+ terminals were also found in the corpus striatum, the amygdala, the SC, the nuclei of the lateral lemniscus and superior olive (Fig. 3B–D). The strongest projections appeared to be in the corpus striatum, which is known to receive a dense AC input that includes L5 (Znamenskiy and Zador 2013; Ponvert and Jaramillo 2019; Bertero et al. 2020) and branches from corticocollicular axons (Moriizumi and Hattori 1991; Asokan et al. 2018). Both dense plexi of terminals and axons en passant were seen (Fig. 3B). Terminal density was lower in the amygdala, SC, nuclei of lateral lemniscus and superior olivary complex (SOC). The distribution of labeled terminals in a single representative animal is seen in Fig. 3E. We did not observe terminal staining in the cochlear nucleus (Fig. 3F), which is a known target of AC-derived corticofugal axons (Weedman and Ryugo 1996a, 1996b; Meltzer and Ryugo 2006). In addition, no labeled terminals were seen in the contralateral AC (Fig. 3G) or other cortical regions. No labeled terminals were seen more caudally than the superior olive.

L6 corticocollicular neurons branch extensively to subcortical sites

To determine which other brain regions receive branching terminals from L6 corticocollicular axons, analogously to above, injections of a Cre-dependent retrograde tracer that induces flippase expression (Cav-FlxFlp) were made into the IC of eight mice that expressed Cre-recombinase in FOXP2+ neurons (Fig. 4A, $n = 8$, age range 3–6 months, 4 female). As expected, labeled terminals were found in the IC, mostly in the most distal rim of the IC, and outside of modules in the LC (Fig. 4B), consistent with previous work (Yudintsev et al. 2021). In the AC, consistent with previous reports, the L6 corticocollicular cells were isolated to the deepest regions of L6, adjacent to the white matter with extensive local branching extending near to L2/3 (Schofield 2009; Slater et al. 2013, 2019). Quantification of layer assignment revealed that this experimental approach labels nearly exclusively L6 neurons in the AC (96.5% labeled neurons in L6, Fig. 4D), suggesting that most mCherry-labeled terminals identified are derived from L6. In mice that also had FG injected into the IC, mCherry-filled L6 neurons were found to be a subset of FG-labeled neurons in L6, but not L5 (Fig. 4E). In FOXP2-Cre animals without Cav-FlxFlp injected into

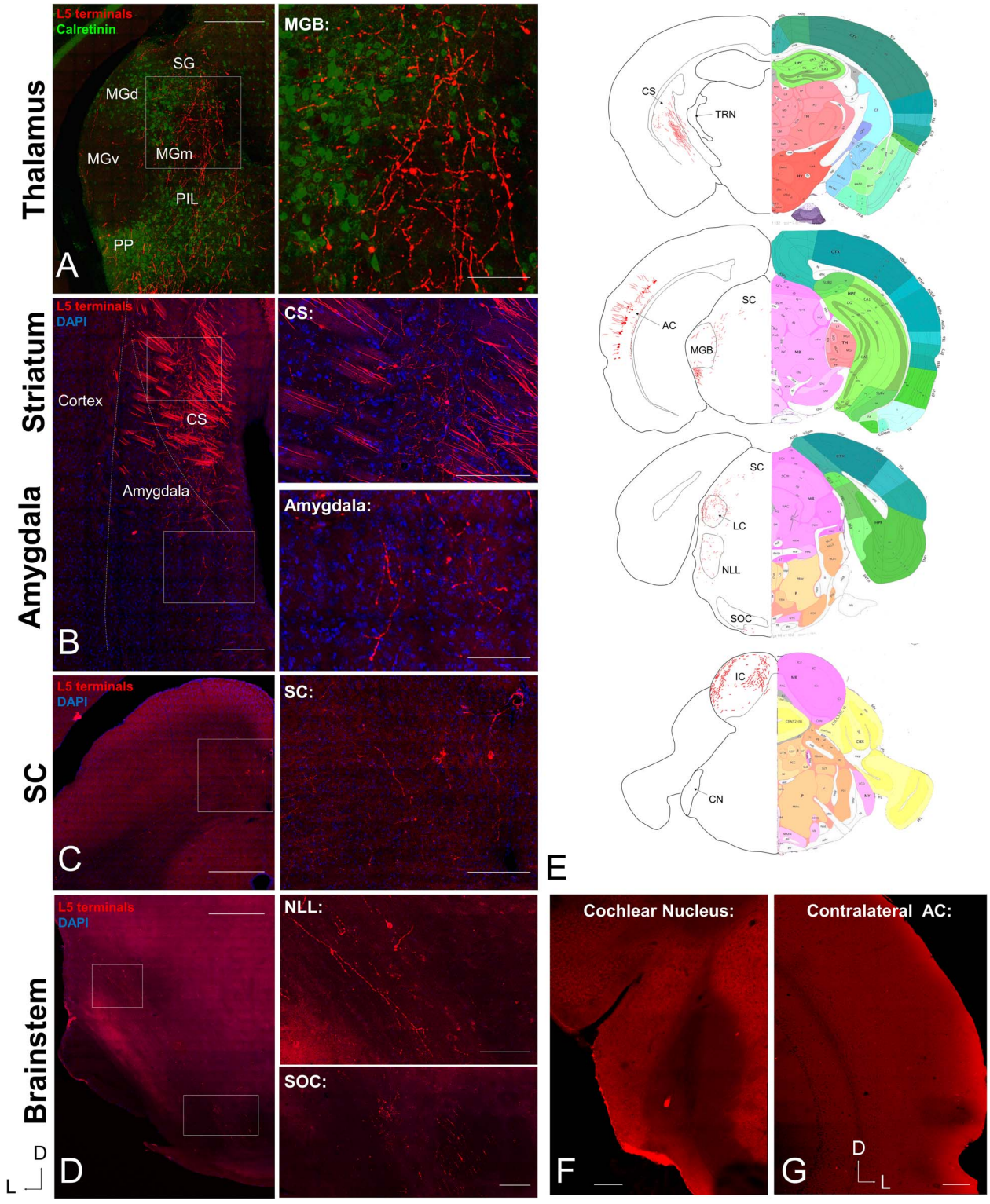

Fig. 3. Non-IC targets of L5 corticocollicular cells. Right column of A–D contains expanded views of boxed areas in left column. Representative sections are shown from the auditory thalamus A) and striatum and amygdala B), SC C), nuclei of the lateral lemniscus and superior olivary nuclei D). Immunostaining for CR was used to delineate the main auditory thalamic nuclei, and DAPI was used as a counterstain for the rest of the images. Scale bar on left = 250 μm, scale bar on right = 50 μm. E) Diagram of labeled cells and axons from a single representative mouse from rostral to caudal. Half-images on the right are derived from Allen Brain Atlas (https://mouse.brain-map.org). Cells and axons are labeled in red. F) Section through the cochlear nucleus ipsilateral to the injection sites, showing no label. G) Section through the AC contralateral to the injection sites, showing no label. No DAPI overlay is included in f and g to facilitate inspection of the images for label. Scale bar for f and g = 200 μm. MGd/m/v, dorsal, medial, or ventral region of the MGB; PIL, posterior intralaminar nucleus; NLL, nuclei of the lateral lemniscus.

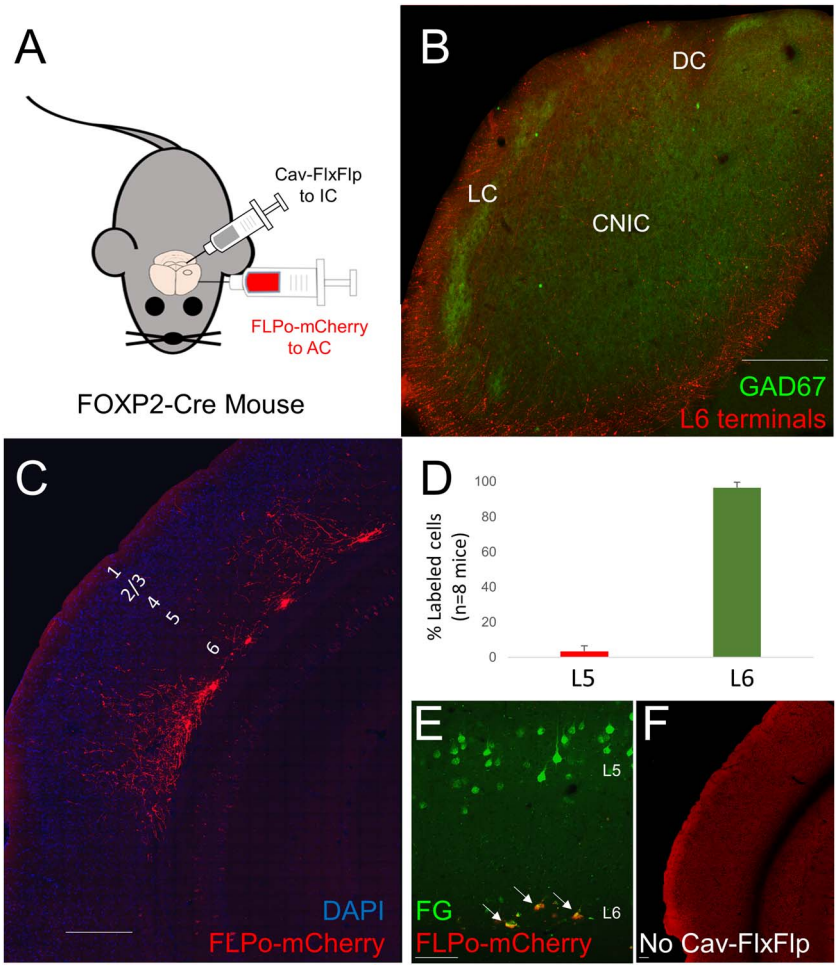

Fig. 4. Experimental setup for examination of L6 corticocollicular branches. A) FOXP2-Cre mice were injected with a combination of Cav-FlxFlp in the IC to induce flippase expression in RBP4+ corticocollicular neurons. The mice were also injected with Flpo-mCherry to induce mCherry expression in the flippase-labeled cells. B) Micrograph of the resulting labeling in the IC showing mCherry terminals in the superficial-most regions of the LC, with a smaller contribution to the DC. Scale bar = 250 μm. C) Retrogradely labeled neurons in L6 of the AC. D) Proportion of L5-labeled vs. L6-labeled cells in the AC across $n = 8$ animals. Scale bar = 300 μm. E) FG-retrogradely labeled cells after IC injection double-labeled with mCherry only in L6 of FOXP2-Cre animals. Double-labeled cells are denoted with white arrows. F) AC of FOXP2-Cre animal injected with Flpo-mCherry but not Cav-FlxFlp showing no signal. Scale bar for E and F = 100 μm.

the IC but with AAV9-Ef1a-fDIO-mCherry into the AC, no AC label was seen (Fig. 4F).

Outside of the IC, dense staining was also observed in the MGB, primarily in the nonlemniscal subdivisions (Fig. 5A). The L6-derived staining in the MGB was more dense than that seen in L5-derived terminals from RBP4-Cre mice (compare to Fig. 3A). Terminals were also seen in the striatum and sparsely in the amygdala (Fig. 5B and C). Sparse terminals were also seen in the nuclei of the lateral lemniscus. The TRN, which is a major target of L6 corticothalamic neurons (Conley et al. 1991; Zhang and Jones 2004; Kimura et al. 2005; Ibrahim et al. 2021), also received dense terminals from L6 corticocollicular branches (Fig. 5E). Very sparse labeling was seen in the deep layers of SC. There was also no labeling observed in the superior olive, or anywhere caudal to the nuclei of the lateral lemniscus The distribution of labeled terminals in a single representative animal is seen in Fig. 5E. We note that some retrogradely labeled cells were typically labeled in the posterior portions of the somatosensory cortex. This finding is consistent with the broader and multisensory input from L6 to the IC than L5, described previously (Yudintsev et al. 2021). We did not observe terminal staining in the cochlear nucleus (Fig. 5F), and no labeled terminals were seen in the contralateral AC (Fig. 5G) or other cortical regions.

L5 and L6 axonal distributions differ across subcortical targets

For $n = 5$ mice in each group, data were available to compute axonal densities across all subcortical targets of branches from L5 or L6 corticocollicular neurons. Axons from L5-derived corticocollicular projections were found across the amygdala, anterior pretectal nucleus (APT), brachium of the inferior colliculus (BIC), corpus striatum, dorsal lateral geniculate nucleus (dLG), IC, lateral lemniscus, lateral posterior nucleus (LP) of thalamus, MGB, SC, SOC, TRN, ventrobasal complex, and ventral lateral geniculate nucleus. The distributions of the percentages of axonal density in each brain region from L5 or L6 are shown in Fig. 6. The largest percentage of axons from L5 (mean = 42.1%, SD 16.7%) was found in the IC. Axons from L6-derived corticocollicular projections were found across the same targets except that no axons were seen in the APT or SOC. The largest percentage of axons from L6 (mean = 33.5%, SD 12.1%) was found in the corpus striatum. A

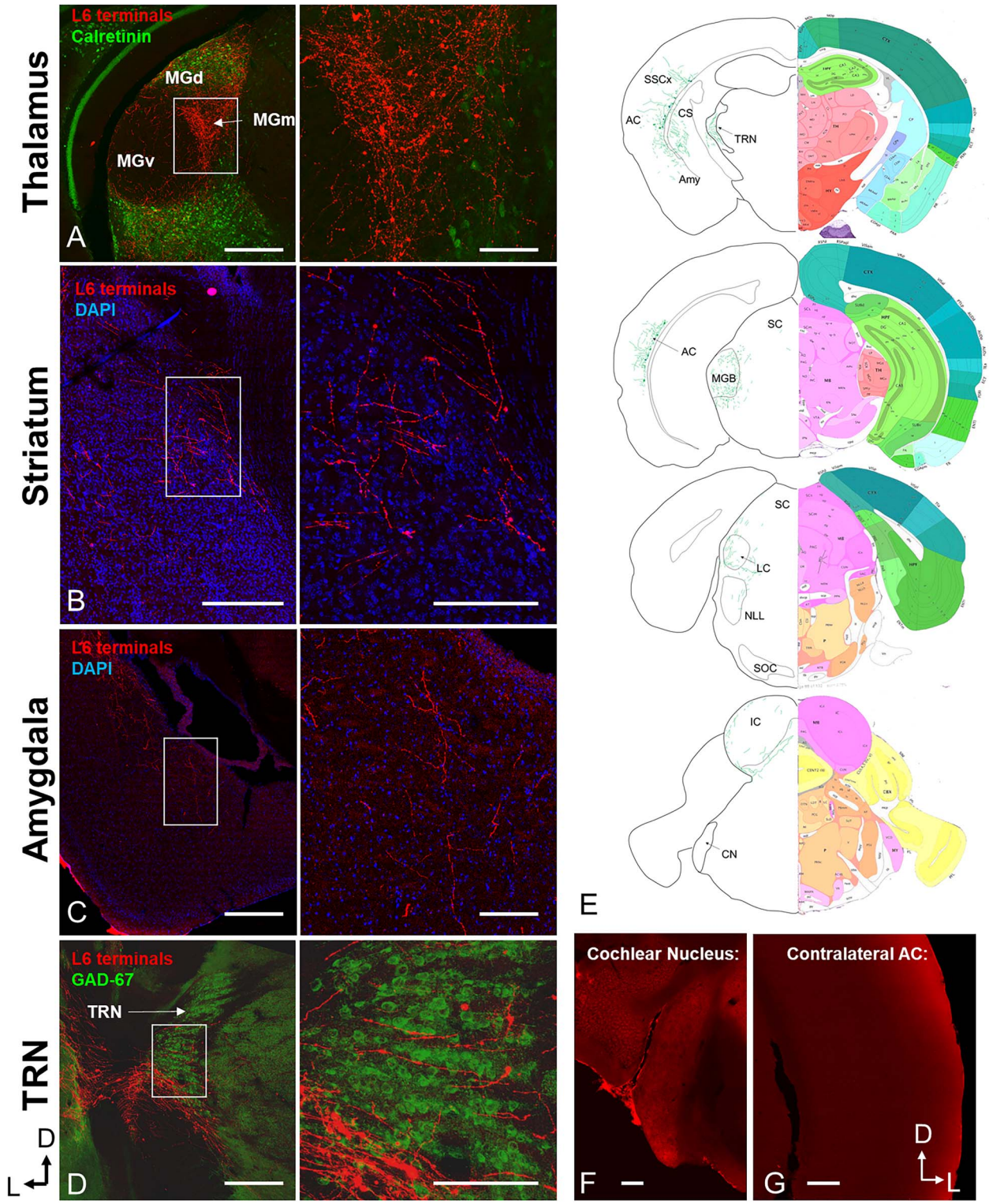

Fig. 5. Non-IC targets of L6 corticocollicular cells. Right column contains expanded views of boxed areas in left column. Representative sections are shown from the auditory thalamus A) and striatum B), which received the most dense inputs, as well as the amygdala C) and TRN D). Immunostaining for CR was used to delineate the main auditory thalamic nuclei, GAD-67 was used to identify the TRN and DAPI was used as a counterstain for the rest of the images. Scale bar on left = 250 μm, scale bar on right = 50 μm. E) Diagram of labeled cells and axons from a single representative mouse from rostral to caudal. Half-images on the right are derived from Allen Brain Atlas (https://mouse.brain-map.org). Cells and axons are labeled in green. F) Section through the cochlear nucleus ipsilateral to the injection sites, showing no label. G) Section through the AC contralateral to the injection sites, showing no label. No DAPI overlay is included in F and G to facilitate inspection of the images for label. Scale bar for F and G = 200 μm.

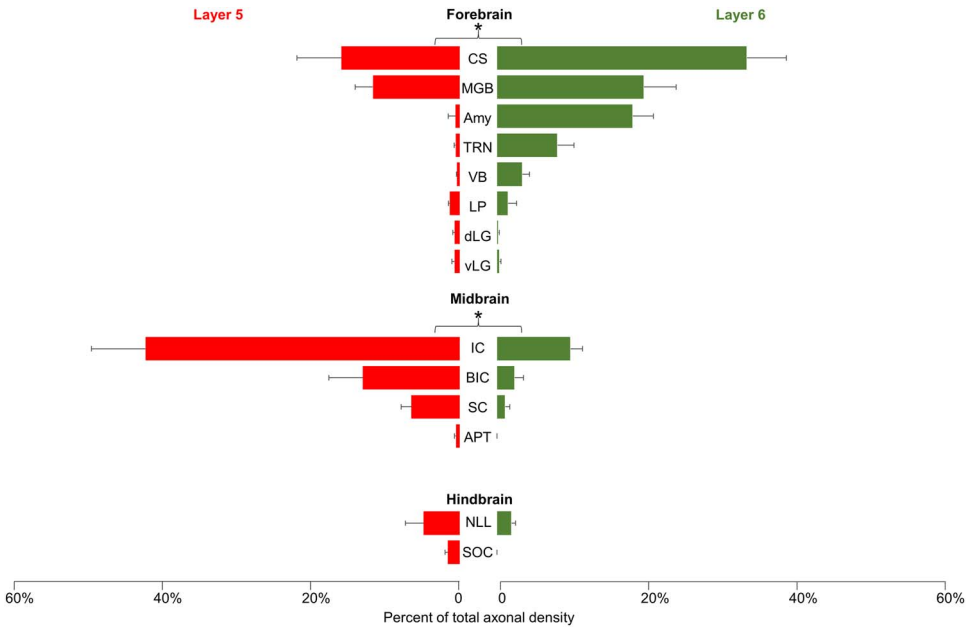

Fig. 6. Butterfly plot showing the mean percentage of axonal density per brain region in RBP4-Cre mice (left) and FOXP2-Cre mice. Brain regions are grouped as being part of the forebrain, midbrain or hindbrain. A two-way ANOVA revealed significant differences in axonal densities across subcortical targets ($F = 21.699$, df = 13, $p < 0.001$) as was as target by layer interactions ($F = 10.453$, df = 13, $P < 0.001$). Pooled densities from forebrain, midbrain, and hindbrain showed significant differences between L5- and L6-derived axonal densities in the forebrain and midbrain, denoted with asterisks. Amy = amygdala, CS = corpus striatum, VB, ventral basal nuclei.

two-way ANOVA revealed significant differences in axonal densities across subcortical targets ($F = 21.699$, df = 13, $P < 0.001$) as was as target by layer interactions ($F = 10.453$, DF = 13, $p < 0.001$). Grouping the targets into brain regions of forebrain, midbrain, and hindbrain, significant differences were seen in L5- vs. L6-terminals in forebrain (L5 = 31.6% (SD 19.3%), L6 = 84.8% (SD 4.5%), $P = 0.008$, Mann–Whitney) and midbrain (L5 = 62.0% (SD 18.1%), L6 = 13.3% (SD 4.0%), $p = 0.008$, Mann–Whitney). Similar low proportions were seen in the hindbrain (L5 = 6.4% (SD 5.8%), L6 = 1.9% (SD 1.3%), $p = 0.10$, Mann–Whitney). Thus, L5-derived corticocollicular axons tend to send the majority of their branches back toward the midbrain, whereas L6-derived corticocollicular axons tend to send their axons toward forebrain structures (thalamus, corpus striatum, and amygdala).

Morphological and chemical signatures of L5 and L6 corticocollicular neurons

Five representative neurons from L5 and from L6 were reconstructed from individual 50 μm sections and shown in Fig. 7A. L5 corticocollicular neurons are large pyramidal neurons with thick apical dendrites with an apical tuft, as has been described previously in L5 subcortically-projecting neurons both in auditory and non-auditory systems (Kasper et al. 1994; Llano and Sherman 2009; Slater et al. 2013; de Kock et al. 2021). L6 corticocollicular neurons are located deep in L6 and are mostly non-pyramidal in shape, with a stellate morphology and heavy local axonal branching, but without extensions into the upper cortical layers. In addition to FOXP2, several markers such as complexin-3 (Hoerder-Suabedissen et al. 2009; Viswanathan et al. 2017), thought to be a marker of subplate neurons as well as NTSR1, have been described in L6 (Guo et al. 2017; Clayton et al. 2021; Ibrahim et al. 2021), whereas Ctip2 has been described in both L5 and L6 (Chang and Kawai 2018). To determine if these markers are present in L5 and/or L6 corticocollicular neurons, retrograde labeling with FG was combined with either immunostaining for these markers or Cre-based expression in the case of NTSR1.

We observed that 49.5% of L5 (323/653 cells, $n = 2$ mice) and 77.3% of L6 (109/141 cells, $n = 2$ mice) corticocollicular cells co-labeled with Ctip2 (Fig. 7B), generally consistent with previous findings demonstrating that a substantial proportion of L5 and L6 corticocollicular projects express this transcription factor (Chang and Kawai 2018). In contrast, complexin-3, though localized to a similar portion of lower L6 as corticocollicular neurons, was found in very few L6 corticocollicular neurons (5.0%, 9/181 cells, $n = 2$ mice, Fig. 7C). In addition, 26.9% of L6 corticocollicular neurons also labeled with NTSR1 (32/119 cells, $n = 2$ mice, Fig. 7D). Consistent with this finding, injection of a Cre-dependent tracer into the AC of NTSR1-Cre mice produced terminal labeling in superficial portion of the IC (Fig. 7E), similar to that seen with FOXP2-Cre mice.

L5 and L6 axons and have different terminal location and size and distributions

To compare L5- and L6-derived axons in the same mice, we took advantage of the selectivity of AAVrg virus to avoid retrograde labeling of L6 (Tervo et al. 2016; Kirchgessner et al. 2021). Thus, when injected into the IC, this approach will selectively label L5 corticocollicular neurons in the AC, which, as shown above, branch extensively to multiple subcortical targets. Using an AAVrg that induced flippase expression in retrogradely labeled cells allowed visualization of L5 neurons by injection of a flippase-dependent mCherry into the AC. By performing these experiments in FOXP2-Cre mice and by injecting flippase-dependent mCherry and Cre-dependent eGFP from the same pipette in the AC, we were able to achieve highly selective L5 (mCherry) and L6 (eGFP) labeling in the same animal in similar regions of the AC (Fig. 8A and B). We used this approach in $n = 4$ mice (2 female) and found excellent layer-specificity in each mouse. As shown in Fig. 8C, we

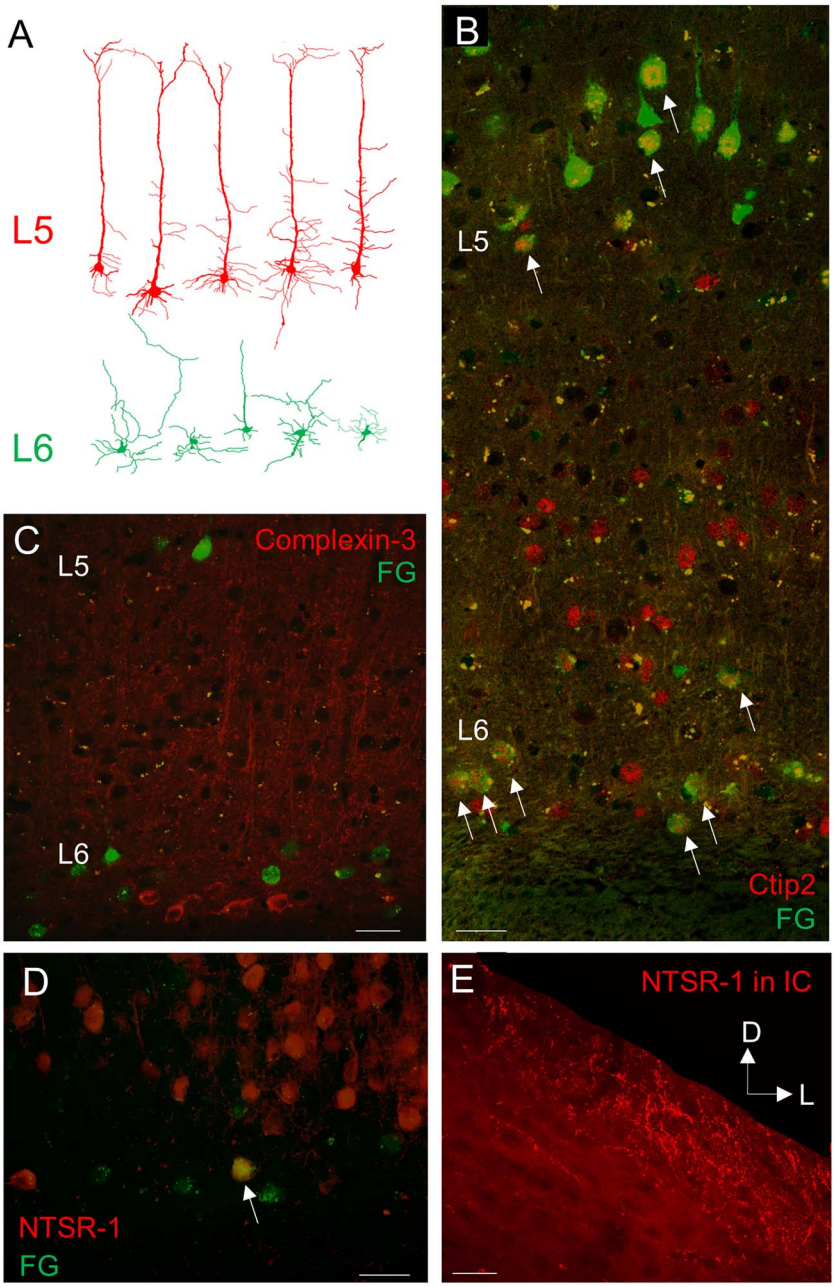

Fig. 7. A) Reconstructions of 5 representative L5 and L6 corticocollicular neurons. B) Representative overlay image showing FG-backlabeled L5 and L6 corticocollicular neurons (green) and immunostaining for Ctip2 (red). C) Representative overlay image showing lack of double-labeled L6 cells after staining FG-backlabeled (green) section for complexin-3 (red). D) Representative overlay image of NTSR1+ neurons (red) and retrogradely labeled FG+. White arrows in all cases correspond to double-labeled cells. E) Axonal and terminal labeling in the LC after Cre-dependent viral injection into the AC of NTSR1-Cre mouse. Scale bars = 50 μm.

observed that ~99% of all labeled cells in the AC were in the expected layer (i.e., red cells in L5 and green cells in L6).

Using this approach, we observed L5- and L6-derived terminals in multiple regions, most densely in the IC, MGB, and striatum, with less dense dual staining in the amygdala, SC, and nuclei of the lateral lemniscus. We examined the distributions of these terminals and, in regions where both L5- and L6-derived terminals were present, measured their cross-sectional areas. We found that in the IC, L6-derived terminals were found in the distal rim of the IC, whereas more dense label was found from L5, which again avoided GABAergic modules and was found through all layers of the LC and more densely in the DC (Fig. 8D–F).

Labeled terminals showed both complementary and overlapping distributions in other brain regions. For example, in the MGB, L6 terminals were found densely in all regions but primarily in the MGv, whereas L5 terminals were found more densely in the MGd and MGm as well as the reported locations of suprageniculate, posterior intralaminar, and peripeduncular nuclei (Fig. 9A). The distributions of terminals from L5 and L6 overlapped substantially in the striatum and AMY, with a larger number of L6 terminals in the AMY, possibly related to the fact that L6-derived neurons were not preselected as being branches from corticocollicular neurons (Fig. 9B and C). Overlapping projections were found in the deep layers of the SC (SCdeep), though, similar to the L6 projections

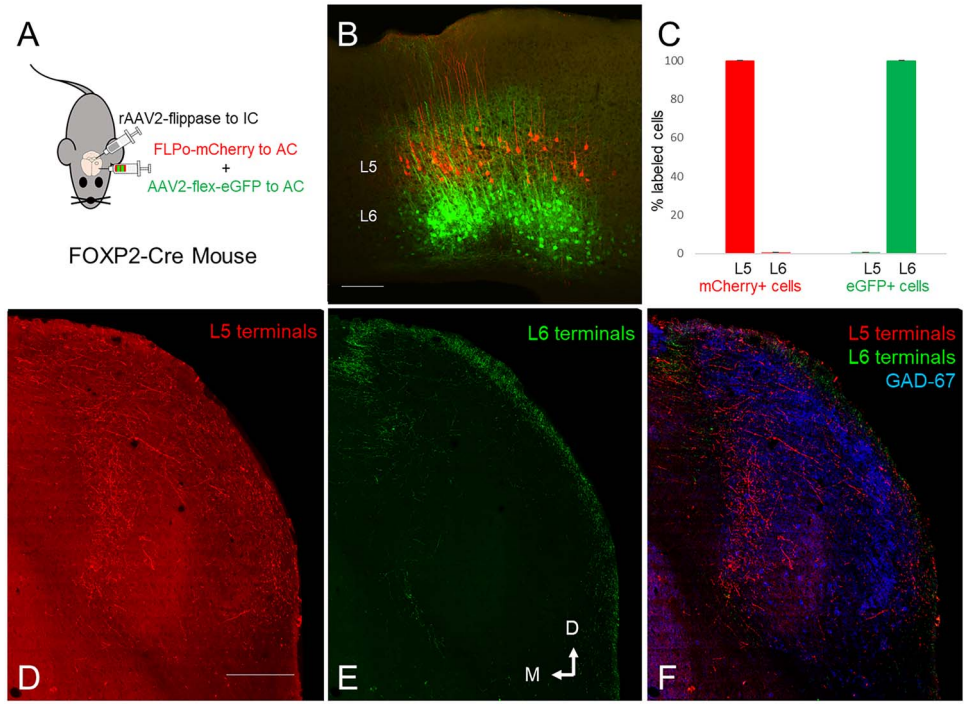

Fig. 8. Experimental setup for examination of L5 and L6 corticofugal projections in the same animal. A) FOXP2-Cre mice were injected with flippase-inducing AAVrg to the IC, which selectively labels L5 neurons. A combination of flippase-dependent mCherry and Cre-dependent eGFP was injected in the AC in the same pipette. B) Representative AC section showing mCherry-labeled cells in L5 and eGFP-labeled cells in L6. C) Quantification of expression either label in or layer ($n = 4$) in the AC showing the high specificity of this approach. D, E) Representative section showing L5-derived mCherry+ terminals across the LC and DC, and L6-derived eGFP+ terminals in the distal rim of the DC and LC, respectively. F) Overlay of E and F, now including GAD-67 immunostaining to show the modules in the LC, showing that both L5- and L6-derived terminals in the LC are primarily in the matrix. Scale bars = 250 μm.

to the IC, there is a rim of L6-derived terminals in the superficial aspect of the SC (Fig. 9D). L6 terminals were present in the nuclei of LL (Fig. 7E), and as expected, few L6-derived terminals were seen in the SOC. In contrast, L5-derived terminals, but no L6-derived terminals were found in the SOC.

To allow a direct comparison of morphologies from terminals derived from each layer, we measured the cross-sectional areas of terminals found in overlapping regions in LC, DC, MGBd, SC, and striatum. In all regions, significant differences in the distributions of terminal size were found, with larger sizes observed in L5-derived terminals. See example from MGd in Fig. 8A and cumulative histograms in Fig. 10B–F. In all cases, significant differences ($p < 0.05$, Mann–Whitney) were seen in the terminal area between L5- and L6-derived terminals. Closer inspection of the distributions of terminal size revealed broad overlap in the proportion of terminals $< 1\ \mu m^2$; however, in all cases, L5-derived terminals had a long tail of large terminals, in many cases extending out to about $8\ \mu m^2$. These data suggest that the differences in average terminal size are driven by a subpopulation of very large terminals derived from L5, but not found in axons from L6 neurons.

Discussion

Summary of results

In the current study, we observed that (i) a subpopulation of both L5 and L6 neurons are double-labeled after injections of retrograde tracers in IC and MGB, suggesting that at least a subpopulation of cells in each layer branch to both structures, (ii) intersectional labeling of RBP4+ L5 or FOXP2+ L6 corticocollicular neurons revealed widespread branching of neurons from both layers to thalamus, striatum, amygdala, SC, and nuclei of lateral lemniscus and in the case of L5, to the SOC, and in the case of L6, to TRN, and (iii) dual labeling of L5 and L6 neurons in the same animal revealed overlapping and complementary distributions of terminal location and size, with the most salient finding being that L5-derived axons contain a subpopulation of giant terminals in all of their targets. Furthermore, the current study represents the first demonstration that L6 corticothalamic projections branch to the IC and that L6 corticocollicular neurons are distinct from subplate neurons found in the same sublayer, as indicated by the absence of complexin-3 staining (Fig. 7C; Hoerder-Suabedissen et al. 2009; Viswanathan et al. 2017). These findings suggest that both L5 and L6 corticocollicular neurons send previously under-recognized widespread branches throughout subcortical regions and that projections from each layer act as partially overlapping and complementary systems.

Technical considerations

All methods to quantify the proportion of neurons that branch to two or more structures have their limitations. The traditional gold standard approach of single-cell filling and axonal reconstructions is a low-throughput approach. Dual-retrograde labeling can label larger numbers of neurons, but has been established to significantly undercount branching axons (Schofield et al. 2007). In the current study, a relatively small proportion of neurons in the AC were found to be double-labeled (highest proportion = 27.6%). We attempted to estimate the degree of double-labeling that was possible using FG and CTB and found an empirically derived maximum of 55.3% as determined in this study by co-injection of FG and CTB into the IC. It is not yet known how the specific projection fields of corticofugal neurons in MGB and IC are related. Presumably, the projection fields of corticofugal axons are spatially restricted such that large injections that fill the MGB and IC (which would likely lead to intolerable spillover to adjacent

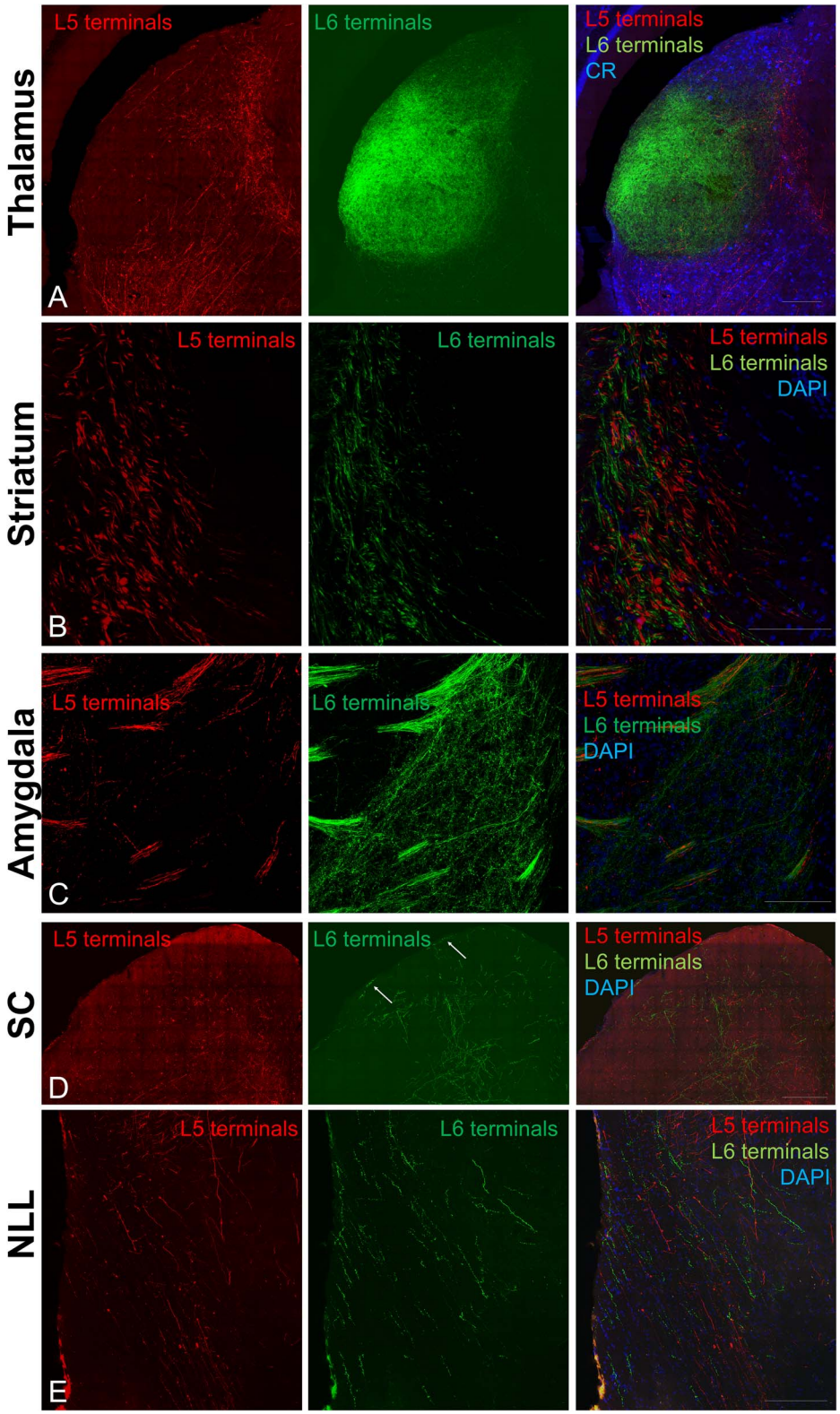

Fig. 9. Non-IC targets receiving both L5 and L6 terminals. Sections are shown from the thalamus A), striatum B), AMY C), SC D), and VNLL E). Left-most column shows L5-derived mCherry-expressing terminals. The middle column shows L6-derived eGFP-expressing terminals the right column shows their overlay with blue counterstain (CR immunostain for thalamus to reveal auditory thalamic subnuclei or DAPI for the rest). Arrows in middle panel of D correspond to superficially located L6-derived terminals in the SC.

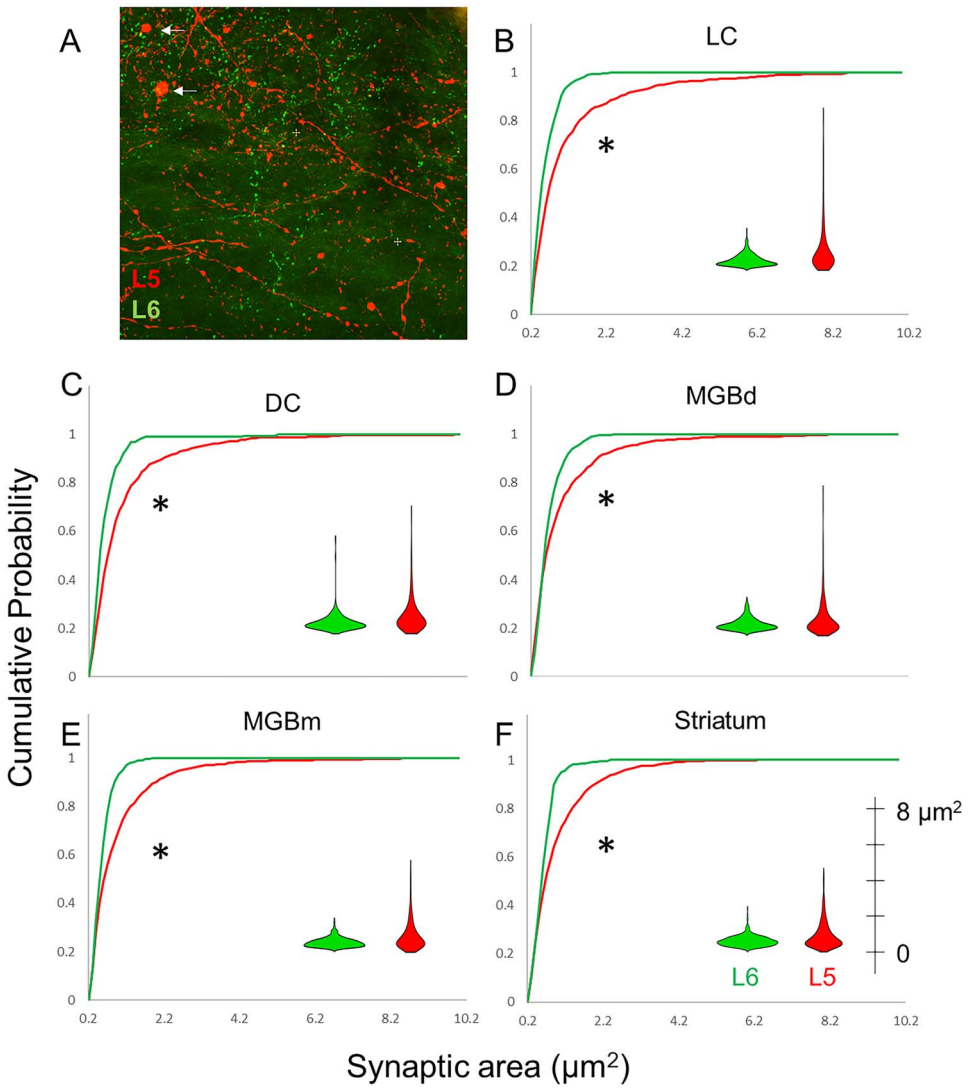

Fig. 10. Terminal size distributions from brain regions receiving both L5 and L6 inputs. A) Representative high-powered section from the MGBd showing a small number of very large L5-derived mCherry expressing terminals intermixed with a large number of small red and small L6-derived eGFP-expressing terminals. B–F) Cumulative histograms of terminal size area across several brain regions receiving both L5 and L6 input. Overlaid are violin plots to assist in the comparison of the distributions of the terminal sizes from both layers. *$p < 0.05$ using Mann–Whitney test. Scale bar = 20 μm.

regions) would be necessary to reveal the extent of branching. Thus the presence of dual-labeled cells should be seen only as evidence for the presence of branching, not an indication of their extent. As such, the lack of quantification of branching should be seen as a limitation in the current study.

This study relied heavily on the presence of RBP4 expression in L5 and FOXP2 expression in L6 to label these populations of cells. It is unlikely that "ectopic" expression of these markers (i.e., FOXP2 in L5 or RBP4 in L6) influenced our results given that we observed > 95% specificity of expression. However, it is possible that these markers may fail to label a subset of corticofugal neurons, thus leaving open the possibility that non-FOXP2+ cells in L6 or non-RBP4+ cells in L5 may have different trends than those seen here. Indeed, roughly 20–30% of L5 and L6 corticocollicular neurons are RBP4- or FOXP2-negative, respectively (Xiong et al. 2015; Yudintsev et al. 2021). We think that this possibility is unlikely to impact our results at least for L5, because the AAVrg experiments that labeled L5 neurons did not rely on RBP4, but revealed nearly identical projection patterns as seen in the Cav-FlxFlp experiments that relabeled RBP4+ neurons. Future work should examine the patterns of branching in RBP4- and FOXP2-negative corticocollicular neurons if/when additional markers for these neurons are discovered.

We also note that comparisons made between L5 and L6 terminals in AAVrg-injected mice carry the proviso that L5-derived axons are all branches of corticocollicular neurons, whereas L6-derived axons are defined only by their expression of FOXP2. Thus, it is possible that differences in termination patterns in non-IC targets may be a reflection of differences in branched vs. unbranched axons rather than a layer-specific difference. We think that this is unlikely to impact the overall trends in the data, particularly on terminal size, given that our data comport well with previous comparisons of L5 vs. L6 terminals using more conventional approaches (Llano and Sherman 2008; Yudintsev et al. 2021). Future work using crosses between mice with flippase (or equivalent non-Cre-recombinase) expression in L5 or L6 (once available) will be able to yield more comparable analysis.

In addition, it should be emphasized that no attempt was made in this study to isolate midbrain injections to IC subnuclei or to intersectionally label cells only to primary AC. The injected

volumes were spread over more than one site in each structure to attempt to achieve uniform labeling, limiting the specificity of the approach. Thus, it is not possible based on the current dataset to determine if branching patterns differ depending on which subnuclei were targeted or which regions of the AC expressed the fluorescent labels. Future work using more focal injections coupled with anatomical and/or physiological subregion markers will be useful to answer this question. In addition, with the current study design, it is neither possible to determine if individual axons branch to innervate more than two targets, nor the proportion of branched vs. unbranched axons in the corticocollicular system. Either triple (or more)-injection retrograde tracing experiments, or detailed axonal reconstructions would be needed to identify broader branching patterns.

Implications of the current study

In this study, we observed that both L5 and L6 corticocollicular projections branch widely to innervate most of the known subcortical targets of the AC. Although many previous studies have individually examined the properties of the projections of the AC to the thalamus, striatum, amygdala, SC, IC, and auditory brainstem (reviewed in Asilador and Llano 2021), the current study links these projections into layer-of-origin-defined systems. That is, it is likely that cortical messages from either L5 or L6 sent to one subcortical target are highly similar to those sent from the same layer to another subcortical target. Thus, rather than considering the separate roles of corticofugal projections to each target based on the target's presumed role in information processing (e.g., cortico-amygdala projections for emotional processing, cortico-striatal for movement, etc.), it may be that a more unified, but as yet unidentified, role exists for each set of layer-derived corticofugal projections. It is also clear from the current data that corticofugal projections are distinct from cortico-cortical projections as no branches of corticofugal axons were seen in distal cortical regions or contralateral AC (Figs 3G and 5G). This finding is generally consistent with the intra-telencephalic vs. extra-telencephalic (i.e., corticofugal) projection dichotomy seen in cortical neurons (Yamawaki and Shepherd 2015; Saiki et al. 2018, reviewed in Baker et al. 2018; Moberg and Takahashi 2022), though exceptions do exist in the striatum, which is innervated by both sets of L5 cells (Reiner et al. 2003).

The current study does not rule out the possibility that a heterogeneous mix of branched vs. unbranched neurons reside in both L5 and L6. However, most studies reporting that L5 or L6 comprise collections of separate populations projections have either used multi-retrograde labeling approaches (with their inherent tendency to undercount branches, as described above) or relied on physiological or physiological differences leading to separate categories of projection neurons being defined (Doucet et al. 2002, 2003; Hattox and Nelson 2007). We note that it is not mutually exclusive to have extensive branching as outlined in the current study and to have multiple classes of widely branching corticofugal neurons in either L5 or L6. Indeed, a heterogenous mix of Ctip2-staining in L5 and L6 and multiple morphologies of L6 corticocollicular neurons (Fig. 7) suggest that multiple subtypes of corticocollicular neurons from each layer exist. Thus, the findings in the current study are not incompatible with previous work documenting multiple classes of corticofugal neurons within each layer.

Anatomical and physiological differences between the L5 and L6 corticofugal projections have been well established. One major difference seen between these projections is terminal size distribution. Similar to other studies (Van Horn and Sherman 2004; Prasad et al. 2020), we observed that although the majority of the terminals in each projection system are small ($<1\ \mu m^2$), only L5 projections have a subpopulation of giant terminals that are $>2\ \mu m^2$. In the L5 corticothalamic system, these terminals have been thought to represent "driver" terminals that can elicit spiking in postsynaptic neurons (Reichova and Sherman 2004; Groh et al. 2008; Mease et al. 2016a, 2016b), serve as the first leg of a cortico-thalamo-cortical route of information flow (Theyel et al. 2010), and in the auditory system have been found primarily in nonlemniscal portions of the MGB (Ojima 1994; Bajo et al. 1995; Bartlett et al. 2000; Hazama et al. 2004; Rouiller and Durif 2004; Llano and Sherman 2008). The current study extends this potential driver role to multiple other subcortical targets: amygdala, striatum, IC, and SC. It is not yet known if these large L5 synapses outside of the thalamus also have postsynaptic specializations of driver synapses such as being located on proximal dendrites or being dominated by ionotropic glutamate receptors, which would enhance their ability to elicit postsynaptic spikes.

It was unexpected that L6 corticocollicular projections branch to other subcortical targets. Previous work had indicated that L6 corticocollicular neurons are located more deeply in L6 than L6 corticothalamic neurons and have different morphology (Schofield 2009; Slater et al. 2013). Specifically, L6 corticocollicular neurons tend to be non-pyramidal and many have the long axis of their somata oriented in parallel to the cortical surface, whereas L6 corticothalamic neurons tend to be pyramidal and have the long axis of their somata oriented vertically along the cortical column. The current study confirmed and extended previous work concerning the location and morphology of L6 corticocollicular neurons (Fig. 7A), including previous findings regarding the extensive dendritic branching of these neurons. The presence of axonal branches to thalamus suggests that the L6 corticothalamic system may be more heterogeneous than previously considered, comprising both pyramidal and non-pyramidal cells and different functional roles based on depth.

In addition to differences in terminal morphology, L5 and L6 projections to different subcortical targets differed in terms of their spatial distributions. For example, as previously described using separate L5 and L6 injections in different animals, and now confirmed in the same animal, L5 corticocollicular axons densely innervate matrix regions of the LC and send projections throughout the DC. In contrast, L6 corticocollicular axons innervate primarily the superficial rim of both structures. It is not yet known if these projections target different cell types, or possibly different portions of individual target neurons, but their different distributions suggest different functional roles. In the thalamus, L5 corticothalamic projections target primarily the nonlemniscal regions (MGd, MGm, paralaminar regions, and peripeduncular regions), whereas L6 projections from AC are found throughout the core regions of MGB. Thus, L5 appears to target the "higher-order" parts of the MGB, potentially to drive cortico-thalamo-cortical processing across the AC hierarchy.

Patterns of branching appear to differ in the brainstem compared with other regions. For example, L5 and L6 projections are unpaired in the superior olivary nucleus. L5 corticocollicular axons appear to branch and extensively innervate the nuclei of the lateral lemniscus and the superior olive, consistent with previous work (Doucet et al. 2002). While L6 also projects to the nuclei of lateral lemniscus, no projections were seen more caudally. Interestingly, we did not observe any consistent branching to the cochlear nucleus, despite the known presence of corticofugal projections to this structure (Weedman and Ryugo 1996a, 1996b; Meltzer and Ryugo 2006) and small percentage of

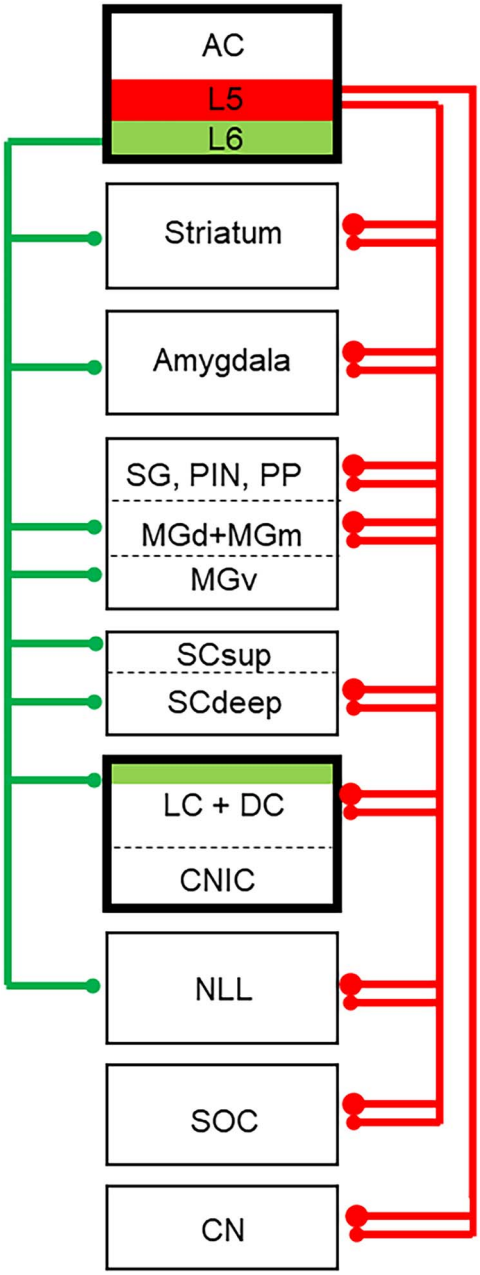

Fig. 11. Summary diagram indicating branching patterns of L5 and L6 corticocollicular neurons. AC and IC are shown in thickened outline to indicate that the current results represent branching from the corticocollicular system. The green rim across the LC + DC indicates that L6 projections target the superficial portions of the IC. The size of the terminal circle indicates whether large or small terminals are found at these sites. All L6 projections end in small terminals, hence small circles. L5 projections end in both large and small terminals, hence large and small circles. The supposition that L5 terminals to the CN end in large and small terminals is supported by Weedman and Ryugo (1996a). SCsup, superficial layers of the SC.

double-labeled cells in AC after dual retrograde injection (10–20%; Doucet et al. 2003). Thus, relative to other subcortical targets of the AC, the cochlear nucleus appears to receive few branches from the corticocollicular system. It is certainly possible that longer incubation times may have revealed these terminals. In addition, the corticobulbar axons to the cochlear nucleus are thin (Weedman and Ryugo 1996a), and may not have labeled in this preparation. That said, a subpopulation of large (2–8 μm in diameter) terminals, along with a large number of small terminals, have been seen the projection from the AC to cochlear nucleus (Weedman and Ryugo 1996b), similar to our L5 findings in other brain region. Thus it is not yet clear based on the current data the degree to which L5 corticocollicular projections branch to cochlear nucleus.

Conclusions

We observed that L5- and L6-derived corticofugal projections from the mouse AC branch widely throughout the brain to innervate striatum, AMY, MGB, SC, IC, and the nuclei of the LL, and in the case of L5, the SOC. In brain regions receiving both L5 and L6 input, their terminal size distributions differ such that a subset of giant terminals is derived from L5, and they show only partial spatial overlap. These findings are summarized in Fig. 11. We have assumed based on the current data that the projection to the cochlear nucleus from L5 is independent of the projections to other subcortical structures. Because our intersectional approach in all cases began with a retrogradely traveling virus injected into the IC, all of the branching described in the current study is indexed to the corticocollicular system. It is not yet known whether other targets of auditory corticofugal pathways (e.g., lateral lemnisus and MGB) are also linked by branching axons. Future work will need to be done to examine such branching patterns.

Overall, these data suggest that the top-down messages being sent by these corticofugal projections are less likely to be specific to a particular target brain region and are instead broadcast to nuclei across several regions along the central auditory hierarchy. Thus, it is interesting to speculate if one of the most well-known roles of corticofugal systems—modulating plastic changes in the tuning of target structures, actually modulate this tuning globally, and not just one structure at a time. Therefore, it may be important to conceive of the corticofugal projections as layer-specific unified systems, rather than individual projections, to fully understand their role in sensory processing.

Acknowledgments

We thank Dr Murray Sherman (University of Chicago) and members of his laboratory for their valuable comments on early versions of this work. We thank Austin Douglas for his technical assistance.

Author contributions

Lina K. Issa (Conceptualization, Data curation, Formal analysis, Investigation, Visualization, Writing—original draft, Writing—review & editing), Nathiya V.C. Sekaran (Data curation, Formal analysis, Investigation, Methodology, Visualization, Writing—review & editing), and Daniel A. Llano (Conceptualization, Data curation, Formal analysis, Funding acquisition, Investigation, Methodology, Project administration, Resources, Supervision, Validation, Visualization, Writing—original draft, Writing—review & editing).

Funding

This work was supported by R01DC016599 and R01DC013073 from the U.S. National Institutes of Health.

Conflict of interest statement: None declared.

Data availability

Data will be made available upon request.

References

Antunes FM, Malmierca MS. Corticothalamic pathways in auditory processing: recent advances and insights from other sensory systems. *Front Neural Circuits*. 2021:15:721186.

Asilador A, Llano DA. Top-down inference in the auditory system: potential roles for corticofugal projections. *Front Neural Circuits*. 2021:14:615259.

Asokan MM, Williamson RS, Hancock KE, Polley DB. Sensory overamplification in layer 5 auditory corticofugal projection neurons following cochlear nerve synaptic damage. *Nat Commun*. 2018:9:1–10.

Bajo VM, Rouiller EM, Welker E, Clarke S, Villa AE, de Ribaupierre Y, de Ribaupierre F. Morphology and spatial distribution of corticothalamic terminals originating from the cat auditory cortex. *Hear Res*. 1995:83:161–174.

Baker A, Kalmbach B, Morishima M, Kim J, Juavinett A, Li N, Dembrow N. Specialized subpopulations of deep-layer pyramidal neurons in the neocortex: bridging cellular properties to functional consequences. *J Neurosci*. 2018:38:5441–5455.

Bartlett E, Stark J, Guillery R, Smith P. Comparison of the fine structure of cortical and collicular terminals in the rat medial geniculate body. *Neuroscience*. 2000:100:811–828.

Bertero A, Zurita H, Normandin M, Apicella AJ. Auditory long-range parvalbumin cortico-striatal neurons. *Front Neural Circuits*. 2020:14:45.

Bourassa J, Deschênes M. Corticothalamic projections from the primary visual cortex in rats: a single fiber study using biocytin as an anterograde tracer. *Neuroscience*. 1995:66:253–263.

Bourassa J, Pinault D, Deschênes M. Corticothalamic projections from the cortical barrel field to the somatosensory thalamus in rats: a single-fibre study using biocytin as an anterograde tracer. *Eur J Neurosci*. 1995:7:19–30.

Chang M, Kawai HD. A characterization of laminar architecture in mouse primary auditory cortex. *Brain Struct Funct*. 2018:223:4187–4209.

Christophe E, Doerflinger N, Lavery DJ, Molnár Z, Charpak S, Audinat E. Two populations of layer V pyramidal cells of the mouse neocortex: development and sensitivity to anesthetics. *J Neurophysiol*. 2005:94:3357–3367.

Clayton KK, Williamson RS, Hancock KE, Tasaka G-ı, Mizrahi A, Hackett TA, Polley DB. Auditory corticothalamic neurons are recruited by motor preparatory inputs. *Curr Biol*. 2021:31:310–321.e315.

Conley M, Kupersmith AC, Diamond IT. The organization of projections from subdivisions of the auditory cortex and thalamus to the auditory sector of the thalamic reticular nucleus in Galago. *Eur J Neurosci*. 1991:3:1089–1103.

de Kock CP, Pie J, Pieneman AW, Mease RA, Bast A, Guest JM, Oberlaender M, Mansvelder HD, Sakmann B. High-frequency burst spiking in layer 5 thick-tufted pyramids of rat primary somatosensory cortex encodes exploratory touch. *Commun Biol*. 2021:4:709.

Deschênes M, Bourassa J, Pinault D. Corticothalamic projections from layer V cells in rat are collaterals of long-range corticofugal axons. *Brain Res*. 1994:664:215–219.

Donoghue JP, Kitai S. A collateral pathway to the neostriatum from corticofugal neurons of the rat sensory-motor cortex: an intracellular HRP study. *J Comp Neurol*. 1981:201:1–13.

Doucet JR, Rose L, Ryugo DK. The cellular origin of corticofugal projections to the superior olivary complex in the rat. *Brain Res*. 2002:925:28–41.

Doucet JR, Molavi DL, Ryugo DK. The source of corticocollicular and corticobulbar projections in area Te1 of the rat. *Exp Brain Res*. 2003:153:461–466.

Ferland RJ, Cherry TJ, Preware PO, Morrisey EE, Walsh CA. Characterization of Foxp2 and Foxp1 mRNA and protein in the developing and mature brain. *J Comp Neurol*. 2003:460:266–279.

Glickfeld LL, Andermann ML, Bonin V, Reid RC. Cortico-cortical projections in mouse visual cortex are functionally target specific. *Nat Neurosci*. 2013:16:219–226.

Groh A, de Kock CP, Wimmer VC, Sakmann B, Kuner T. Driver or coincidence detector: modal switch of a corticothalamic giant synapse controlled by spontaneous activity and short-term depression. *J Neurosci*. 2008:28:9652–9663.

Guo W, Clause AR, Barth-Maron A, Polley DB. A corticothalamic circuit for dynamic switching between feature detection and discrimination. *Neuron*. 2017:95:180–194.e185.

Hattox AM, Nelson SB. Layer V neurons in mouse cortex projecting to different targets have distinct physiological properties. *J Neurophysiol*. 2007:98:3330–3340.

Hazama M, Kimura A, Donishi T, Sakoda T, Tamai Y. Topography of corticothalamic projections from the auditory cortex of the rat. *Neuroscience*. 2004:124:655–667.

Hoerder-Suabedissen A, Wang WZ, Lee S, Davies KE, Goffinet AM, Rakić S, Parnavelas J, Reim K, Nicolić M, Paulsen O. Novel markers reveal subpopulations of subplate neurons in the murine cerebral cortex. *Cereb Cortex*. 2009:19:1738–1750.

Hoerder-Suabedissen A, Hayashi S, Upton L, Nolan Z, Casas-Torremocha D, Grant E, Viswanathan S, Kanold PO, Clasca F, Kim Y. Subset of cortical layer 6b neurons selectively innervates higher order thalamic nuclei in mice. *Cereb Cortex*. 2018:28:1882–1897.

Ibrahim BA, Murphy CA, Yudintsev G, Shinagawa Y, Banks MI, Llano DA. Corticothalamic gating of population auditory thalamocortical transmission in mouse. *eLife*. 2021:10:e56645.

Kasper EM, Larkman AU, Lübke J, Blakemore C. Pyramidal neurons in layer 5 of the rat visual cortex. I. Correlation among cell morphology, intrinsic electrophysiological properties, and axon targets. *J Comp Neurol*. 1994:339:459–474.

Kim J, Matney CJ, Blankenship A, Hestrin S, Brown SP. Layer 6 corticothalamic neurons activate a cortical output layer, layer 5a. *J Neurosci*. 2014:34:9656–9664.

Kimura A, Donishi T, Okamoto K, Tamai Y. Topography of projections from the primary and non-primary auditory cortical areas to the medial geniculate body and thalamic reticular nucleus in the rat. *Neuroscience*. 2005:135:1325–1342.

Kirchgessner MA, Franklin AD, Callaway EM. Distinct "driving" versus "modulatory" influences of different visual corticothalamic pathways. *Curr Biol*. 2021:31:5121–5137.e5127.

Kozorovitskiy Y, Saunders A, Johnson CA, Lowell BB, Sabatini BL. Recurrent network activity drives striatal synaptogenesis. *Nature*. 2012:485:646–650.

Lesicko AM, Hristova TS, Maigler KC, Llano DA. Connectional modularity of top-down and bottom-up multimodal inputs to the lateral cortex of the mouse inferior colliculus. *J Neurosci*. 2016:36:11037–11050.

Llano DA, Sherman SM. Evidence for nonreciprocal organization of the mouse auditory thalamocortical-corticothalamic projection systems. *J Comp Neurol*. 2008:507:1209–1227.

Llano DA, Sherman SM. Differences in intrinsic properties and local network connectivity of identified layer 5 and layer 6 adult mouse auditory corticothalamic neurons support a dual corticothalamic projection hypothesis. *Cereb Cortex*. 2009:19:2810–2826.

Mease RA, Sumser A, Sakmann B, Groh A. Cortical dependence of whisker responses in posterior medial thalamus in vivo. *Cereb Cortex*. 2016a:26:3534–3543.

Mease RA, Sumser A, Sakmann B, Groh A. Corticothalamic spike transfer via the L5B-POm pathway in vivo. *Cereb Cortex*. 2016b:26: 3461–3475.

Meltzer NE, Ryugo DK. Projections from auditory cortex to cochlear nucleus: a comparative analysis of rat and mouse. *Anat Rec A Discov Mol Cell Evol Biol*. 2006:288:397–408.

Moberg S, Takahashi N. Neocortical layer 5 subclasses: from cellular properties to roles in behavior. *Front Synaptic Neurosci*. 2022: 14:1006773.

Moriizumi T, Hattori T. Pyramidal cells in rat temporoauditory cortex project to both striatum and inferior colliculus. *Brain Res Bull*. 1991:27:141–144.

Ojima H. Terminal morphology and distribution of corticothalamic fibers originating from layers 5 and 6 of cat primary auditory cortex. *Cereb Cortex*. 1994:4:646–663.

Ponvert ND, Jaramillo S. Auditory thalamostriatal and corticostriatal pathways convey complementary information about sound features. *J Neurosci*. 2019:39:271–280.

Prasad JA, Carroll BJ, Sherman SM. Layer 5 corticofugal projections from diverse cortical areas: variations on a pattern of thalamic and extrathalamic targets. *J Neurosci*. 2020:40:5785–5796.

Reichova I, Sherman SM. Somatosensory corticothalamic projections: distinguishing drivers from modulators. *J Neurophysiol*. 2004:92:2185–2197.

Reiner A, Jiao Y, Del Mar N, Laverghetta AV, Lei WL. Differential morphology of pyramidal tract-type and intratelencephalically projecting-type corticostriatal neurons and their intrastriatal terminals in rats. *J Comp Neurol*. 2003:457:420–440.

Rock C, Zurita H, Wilson C, junior Apicella A. An inhibitory corticostriatal pathway. *eLife*. 2016:5:e15890.

Rouiller EM, Durif C. The dual pattern of corticothalamic projection of the primary auditory cortex in macaque monkey. *Neurosci Lett*. 2004:358:49–52.

Rumberger A, Schmidt M, Lohmann H, Hoffmann K-P. Correlation of electrophysiology, morphology, and functions in corticotectal and corticopretectal projection neurons in rat visual cortex. *Exp Brain Res*. 1998:119:375–390.

Saiki A, Sakai Y, Fukabori R, Soma S, Yoshida J, Kawabata M, Yawo H, Kobayashi K, Kimura M, Isomura Y. In vivo spiking dynamics of intra-and extratelencephalic projection neurons in rat motor cortex. *Cereb Cortex*. 2018:28:1024–1038.

Schofield B. Projections to the inferior colliculus from layer VI cells of auditory cortex. *Neuroscience*. 2009:159:246–258.

Schofield BR, Schofield RM, Sorensen KA, Motts SD. On the use of retrograde tracers for identification of axon collaterals with multiple fluorescent retrograde tracers. *Neuroscience*. 2007:146: 773–783.

Sherman SM. Functioning of circuits connecting thalamus and cortex. *Compr Physiol*. 2011:7:713–739.

Sherman SM, Usrey WM. Cortical control of behavior and attention from an evolutionary perspective. *Neuron*. 2021:109:3048–3054.

Slater BJ, Willis AM, Llano DA. Evidence for layer-specific differences in auditory corticocollicular neurons. *Neuroscience*. 2013:229: 144–154.

Slater BJ, Yudintsev G, Lee CM, Llano DA. Thalamocortical and intracortical inputs differentiate layer-specific mouse auditory corticocollicular neurons. *J Neurosci*. 2019:39:256–270.

Tervo DGR, Hwang B-Y, Viswanathan S, Gaj T, Lavzin M, Ritola KD, Lindo S, Michael S, Kuleshova E, Ojala D. A designer AAV variant permits efficient retrograde access to projection neurons. *Neuron*. 2016:92:372–382.

Theyel BB, Llano DA, Sherman SM. The corticothalamocortical circuit drives higher-order cortex in the mouse. *Nat Neurosci*. 2010:13:84–88.

Van Horn SC, Sherman SM. Differences in projection patterns between large and small corticothalamic terminals. *J Comp Neurol*. 2004:475:406–415.

Viswanathan S, Sheikh A, Looger LL, Kanold PO. Molecularly defined subplate neurons project both to thalamocortical recipient layers and thalamus. *Cereb Cortex*. 2017:27:4759–4768.

Wang Z, McCormick DA. Control of firing mode of corticotectal and corticopontine layer V burst-generating neurons by norepinephrine, acetylcholine, and 1S, 3R-ACPD. *J Neurosci*. 1993:13: 2199–2216.

Weedman DL, Ryugo DK. Projections from auditory cortex to the cochlear nucleus in rats: synapses on granule cell dendrites. *J Comp Neurol*. 1996a:371:311–324.

Weedman DL, Ryugo DK. Pyramidal cells in primary auditory cortex project to cochlear nucleus in rat. *Brain Res*. 1996b:706: 97–102.

Xiong XR, Liang F, Zingg B, Ji X-Y, Ibrahim LA, Tao HW, Zhang LI. Auditory cortex controls sound-driven innate defense behaviour through corticofugal projections to inferior colliculus. *Nat Commun*. 2015:6:1–12.

Yamawaki N, Shepherd GM. Synaptic circuit organization of motor corticothalamic neurons. *J Neurosci*. 2015:35:2293–2307.

Yudintsev G, Asilador AR, Sekaran NVC, Coppinger M, Nair K, Prasad M, Xiao G, Ibrahim BA, Shinagawa Y, Llano DA. Evidence for layer-specific connectional heterogeneity in the mouse auditory corticocollicular system. *J Neurosci*. 2021:41:9906–9918.

Zhang L, Jones EG. Corticothalamic inhibition in the thalamic reticular nucleus. *J Neurophysiol*. 2004:91:759–766.

Znamenskiy P, Zador AM. Corticostriatal neurons in auditory cortex drive decisions during auditory discrimination. *Nature*. 2013:497: 482–485.

Zurita H, Rock C, Perkins J, Aj A. A layer-specific corticofugal input to the mouse superior colliculus. *Cereb Cortex*. 2018:28:2817–2833.